*Progress In Electromagnetics Research M, Vol. 29, 207–222, 2013*

# ELECTROMAGNETIC WAVE SCATTERING FROM CYLINDRICAL STRUCTURE WITH MIXED-IMPEDANCE BOUNDARY CONDITIONS

**Mostafa Mashhadi*, Ali Abdolali, and Nader Komjani**

College of Electrical Engineering, Iran University of Science and Technology, Narmak, Tehran, Iran

**Abstract**—Recently, a new boundary condition is introduced in which surface shows different impedances for TE and TM electromagnetic fields. This new boundary condition is called mixed-impedance (MI) boundary condition and can be expressed in terms of normal components of electromagnetic fields. In this paper, the cylindrical structures with MI boundary condition were investigated and the scattering of such structures was obtained for both normal and oblique incidence and both $TE_Z$ and $TM_Z$ polarizations. The interesting feature of MI boundary condition was that the boundary conditions of PEC, PMC, DB, D'B', and isotropic impedance boundaries were special cases of the MI boundary. Therefore, by calculating the electromagnetic scattering from a MI boundary, scattering from various boundary conditions could be easily obtained. It was also demonstrated that, by proper choice of boundary conditions the forward or backward RCS (radar cross section) could be significantly increased or decreased.

## 1. INTRODUCTION

Electromagnetic boundary conditions are normally defined in terms of tangential components of electric and magnetic fields. These conventional boundary conditions are listed as follows [1–3].

- Perfect electric conductor (PEC) $\mathbf{n} \times \mathbf{E} = \mathbf{0}$
- Impedance boundary condition $\mathbf{E}_t = \bar{\bar{Z}}_s \cdot \mathbf{n} \times \mathbf{H}$
- Perfect magnetic conductor (PMC) $\mathbf{n} \times \mathbf{H} = 0$
- Perfect electromagnetic conductor (PEMC) $\mathbf{n} \times (\mathbf{H} + M\mathbf{E}) = 0$

*Received 28 December 2012, Accepted 4 March 2013, Scheduled 7 March 2013*

* Corresponding author: Mostafa Mashhadi (mashhadi@elec.iust.ac.ir).

- Soft and hard surface $\mathbf{V} \cdot \mathbf{E} = 0$, $\mathbf{V} \cdot \mathbf{H} = 0$ for $\mathbf{V} \cdot \mathbf{n} = 0$.

where $\mathbf{n}$ is the unit normal vector to the boundary surface, $\mathbf{t}$ represents the tangential field components, $\bar{\bar{Z}}_s$ denotes the two-dimensional surface-impedance dyadic, $M$ denotes the admittance of the PEMC boundary and $\mathbf{V}$ is a real unit vector tangential to the surface.

Recently, a new class of boundary conditions has been introduced in which the boundary conditions are expressed in terms of normal components of the vectors $D$ and $B$. These boundary conditions are named DB, D'B', DB' and D'B surfaces. The boundary conditions in these surfaces are stated as follows [4].

- DB surface $\mathbf{n} \cdot \mathbf{D} = 0$ and $\mathbf{n} \cdot \mathbf{B} = 0$.
- D'B' surface $\nabla \cdot (\mathbf{nn} \cdot \mathbf{D}) = 0$ and $\nabla \cdot (\mathbf{nn} \cdot \mathbf{B}) = 0$.
- DB' surface $\mathbf{n} \cdot \mathbf{D} = 0$ and $\nabla \cdot (\mathbf{nn} \cdot \mathbf{B}) = 0$.
- D'B surface $\nabla \cdot (\mathbf{nn} \cdot \mathbf{D}) = 0$ and $\mathbf{n} \cdot \mathbf{B} = 0$.

In [4], it was demonstrated that, if a given field can be decomposed to TE and TM polarizations with respect to the normal vector to the surface, then, these normal boundary conditions can be replaced with PEC or PMC surfaces for each of TE and TM polarizations. This expression is shown as a summary in Table 1.

**Table 1.** Expressing normal boundary conditions in terms of PEC or PMC surfaces according to the type of polarization.

| | TE | TM |
|---|---|---|
| DB | PEC | PMC |
| D'B' | PMC | PEC |
| DB' | PMC | PMC |
| D'B | PEC | PEC |

It can be seen that the DB' surface acts similar to PMC for both polarization; then DB' boundary condition can be considered corresponding to the PMC boundary. Similarly, D'B surface corresponds to PEC boundary. DB and D'B' boundaries show different behaviors for TE and TM polarizations and can act similar to PEC or PMC surfaces depending on the type of polarization. So far, different methods have been introduced for the realizations of DB and D'B' surfaces [5–10].

In [11], a new anisotropic impedance boundary condition was introduced which was called mixed-impedance (MI) boundary condition, in which a TE/TM decomposition of the field with respect

to the unit normal vector to the boundary surface was assumed and the boundary had two different surface impedances for TE and TM polarized fields.

$$\mathbf{E}_{\mathrm{TE}} = Z_{\mathrm{TE}}\mathbf{n} \times \mathbf{H}_{\mathrm{TE}} \tag{1}$$

$$\mathbf{H}_{\mathrm{TM}} = -\frac{1}{Z_{\mathrm{TM}}}\mathbf{n} \times \mathbf{E}_{\mathrm{TM}} \tag{2}$$

where $Z_{\mathrm{TE}}$ and $Z_{\mathrm{TM}}$ are surface impedances of TE and TM polarized fields, respectively. It was indicated that MI boundary can be expressed as a combination of four normal components of electric and magnetic fields as follows [11].

$$jk\eta\mathbf{n} \cdot \mathbf{H} - Z_{\mathrm{TE}}\nabla \cdot (\mathbf{nn} \cdot \mathbf{H}) = 0 \tag{3}$$

$$jkZ_{\mathrm{TM}}\mathbf{n} \cdot \mathbf{E} - \eta\nabla \cdot (\mathbf{nn} \cdot \mathbf{E}) = 0 \tag{4}$$

The interesting property of MI boundary condition is that PEC, PMC, DB and D'B' surfaces are its specific cases. When $Z_{\mathrm{TE}} = Z_{\mathrm{TM}}$, MI boundary is an isotropic impedance boundary that includes the specific cases of PEC ($Z_{\mathrm{TE}} = Z_{\mathrm{TM}} = 0$) and PMC ($Z_{\mathrm{TE}} = Z_{\mathrm{TM}} = \infty$). Also, for isotropic and homogenous media, $Z_{\mathrm{TE}} = 0$ and $Z_{\mathrm{TM}} = \infty$ corresponds to DB boundary and $Z_{\mathrm{TE}} = \infty$ and $Z_{\mathrm{TM}} = 0$ corresponds to D'B' surface.

The two surface impedances were also expressed in terms of two other parameters of $s$, $a$ [11].

$$Z_{\mathrm{TE}} = \eta(s + a), \quad Z_{\mathrm{TM}} = \frac{\eta}{(s - a)} \tag{5}$$

where $s$ and $a$ are called self-dual and anti-self-dual surface-impedance parameters, respectively. The two parameters of s and a determine whether boundary is a self-dual boundary or not. The concept of self-dual is represented in [12]. [12] states that a medium and/or boundary condition are called self-dual when they remain invariant in the duality transformation. It is shown in [11] that when $a = 0$, MI boundary is a self-dual boundary for all values of $s$. Then $s$ and a are called the self-dual and anti-self-dual surface-impedance parameters.

Until now, only scattering from a MI sphere has been studied [11] and scattering from cylindrical structure with MI boundary has not studied yet. Therefore, in this paper the scattering of cylindrical structures with MI boundary are investigated. Using (3)–(5), boundary conditions in cylindrical structures have the following form.

$$jkH_\rho - (s + a)\frac{1}{\rho}\frac{\partial(\rho H_\rho)}{\partial\rho} = 0 \tag{6}$$

$$jkE_\rho - (s - a)\frac{1}{\rho}\frac{\partial(\rho E_\rho)}{\partial\rho} = 0 \tag{7}$$

where $H_\rho$ and $E_\rho$ are normal components of electric and magnetic fields at the boundary surface.

In Section 2, scattering of a normally incident plane waves from a MI boundary cylinder is investigated. Scattering of an obliquely incident plane wave from a MI boundary cylinder is obtained in Section 3 and the conclusions are given in Section 4.

## 2. SCATTERING OF A NORMALLY INCIDENT PLANE WAVE FROM MI CYLINDER

We know that each plane wave can be expressed as the sum of two plane waves with TM and TE polarizations. Then, by obtaining the scattering fields of a cylinder for both polarizations, the scattering fields of any plane wave can be calculated. So in this section, the scattered fields from MI cylinder for both $\mathrm{TM}_Z$ and $\mathrm{TE}_Z$ polarizations are computed.

### 2.1. Normally Incident Plane Wave: $\mathrm{TM}_Z$ Polarization

Let us suppose that a $\mathrm{TM}_Z$ plane wave is normally incident upon an MI boundary cylinder of radius $\rho_0$, as shown in Fig. 1. According to cylindrical wave transformation, the incident electric field can be expanded by an infinite sum of cylindrical wave functions [13]

$$E_Z^i = E_0 e^{-jkx} = E_0 \sum_{n=-\infty}^{+\infty} j^{-n} J_n(k\rho) e^{jn\varphi} \tag{8}$$

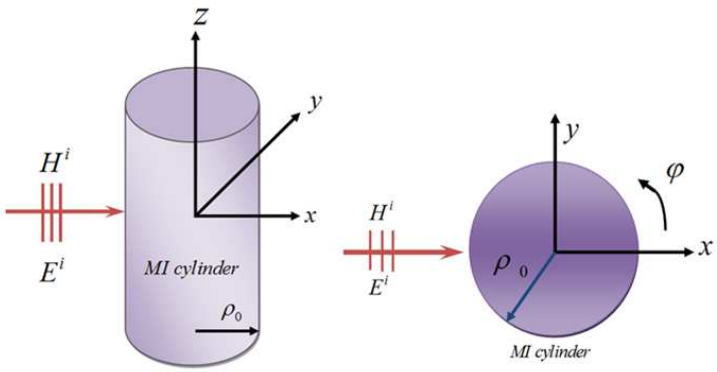


**Figure 1.** Uniform plane wave with normal incidence to MI cylinder.

The scattered electric field from the cylinder can be considered as follows:

$$E_Z^s = E_0 \sum_{n=-\infty}^{+\infty} A_n j^{-n} H_n^2(k\rho) e^{jn\varphi} \tag{9}$$

where $H_n^2(k\rho)$ is the Hankel function of the second kind of order $n$, and $A_n$ represents the unknown coefficient and is determined from the boundary conditions. Since the magnetic field along $z$-axis is zero ($H_z = 0$), it can be shown using Maxwell's equations that only the components of $E_Z$, $H_\rho$ and $H_\varphi$ have non-zero values and the other field components are null.

The radial component of incident and scattered magnetic fields are

$$H_\rho^i = \frac{-1}{j\omega\mu\rho}\frac{\partial E_Z^i}{\partial\varphi} = \frac{-E_0}{\omega\mu\rho}\sum_{n=-\infty}^{+\infty} n j^{-n} J_n(k\rho) e^{jn\varphi} \tag{10}$$

$$H_\rho^s = \frac{-1}{j\omega\mu\rho}\frac{\partial E_Z^s}{\partial\varphi} = \frac{-E_0}{\omega\mu\rho}\sum_{n=-\infty}^{+\infty} n A_n j^{-n} H_n^2(k\rho) e^{jn\varphi} \tag{11}$$

The scattering amplitudes $A_n$ are determined by (10) and (11) and applying the boundary conditions (6).

$$A_n = -\frac{J_n(k\rho_0) + j(s+a)J_n'(k\rho_0)}{H_n^2(k\rho_0) + j(s+a)H_n'^2(k\rho_0)}, \quad n \neq 0 \tag{12}$$

Note that (12) is valid for $n \neq 0$. For $n = 0$ using (10) and (11); therefore, boundary condition is itself satisfied and $A_0$ must be determined in another way. Indeed, for $n = 0$, incident and scattered waves are $\mathrm{TEM}_\rho$, whereas it was assumed that fields can be expressed as a sum of partial fields $\mathrm{TM}_\rho$ and $\mathrm{TE}_\rho$. The coefficient $A_0$ must be determined from additional information. This situation is similar to the TEM wave incident normally to the planar boundary [4]. The additional information is obtained from the way of realization of MI boundary. If it is assumed that the MI cylinder acts like a dielectric cylinder for $\mathrm{TEM}_\rho$ wave that have permittivity and permeability of $\varepsilon_d$ and $\mu_d$, respectively, $A_0$ can be obtained from the following equation.

$$A_0 = -\frac{J_0(k\rho_0) - \frac{\eta_d}{\eta_0}\frac{J_0(k_d\rho_0)}{J_0'(k_d\rho_0)}J_0'(k\rho_0)}{H_0^2(k\rho_0) - \frac{\eta_d}{\eta_0}\frac{J_0(k_d\rho_0)}{J_0'(k_d\rho_0)}H'^2_0(k\rho_0)} \tag{13}$$

By comparing (12) and (13), it is observed that if the values of $\varepsilon_d$ and $\mu_d$ are chosen so that $j(s+a) = -\frac{\eta_d}{\eta_0}\frac{J_0(k_d\rho_0)}{J_0'(k_d\rho_0)}$, $A_0$ can also be calculated by (12).

After calculating the coefficients $A_n$, RCS can be obtained similar to [13]. Assuming that all the coefficients $A_n$ are computed by (12), then the normalized backward RCS (normalized scattering width for $\varphi = 180°$) and normalized forward RCS (normalized scattering width for $\varphi = 0°$) in terms of $(s+a)$ are plotted in Fig. 2. It is observed that normalized forward and backward RCS change in the ranges of 5–35 and 1–5, respectively. The maximum RCS in two directions occurs approximately when $s + a = -j$. Normalized RCS in terms of $\varphi$ for different boundary conditions is plotted in Fig. 3.

Also, by comparing (12) with the coefficients obtained from an impedance cylinder, it can be observed that by selecting $Z_s = \eta_0(s+a)$,

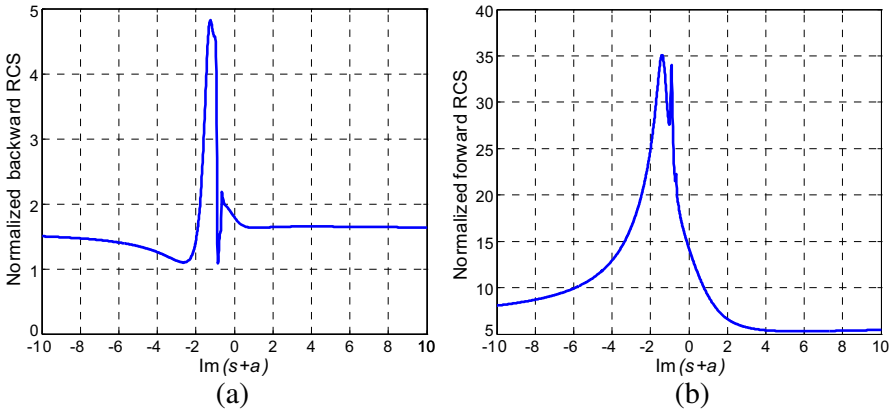


**Figure 2.** Normalized backward and forward RCS as a function of $\mathrm{Im}(s+a)$. $\rho_0 = 0.6\lambda_0$, $\mathrm{Re}(s+a) = 0.02$, is added to make the curves smoother. (a) Normalized backward RCS. (b) Normalized forward RCS.

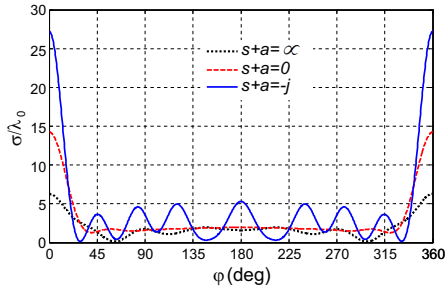


**Figure 3.** Normalized bistatic RCS as a function of $\varphi$ for different values of $(s+a)$, $\rho_0 = 0.6\lambda_0$.

the coefficients $A_n$ in both cylinders will be equal ($Z_s$ is the surface impedance of cylinder). In other words, in normal incidence to the MI cylinder for $\mathrm{TM}_Z$ polarization, MI cylinder acts like an impedance cylinder with the surface impedance of $\eta_0(s+a)$ (it is assumed that the $A_0$ is calculated from (12)). If $A_n$ are computed in special cases of DB ($s = 0$, $a = 0$), D'B' ($s = \infty$, $a = 0$), PEC ($s = -a = \infty$) and PMC ($s = a = \infty$), it will be seen that the coefficients $A_n$ for PEC and DB are the same; also, $A_n$ are equal for D'B' and PMC. Since, for normal incidence, $\mathrm{TM}_Z$ polarization can be considered as $\mathrm{TE}\rho$ polarization (unless $n = 0$). The obtained results are predictable from Table 1.

### 2.2. Normally Incident Plane Wave: $\mathrm{TE}_Z$ Polarization

Incident and scattered fields for $\mathrm{TE}_Z$ polarization can be expressed as follows.

$$H_Z^i = H_0 e^{-jkx} = H_0 \sum_{n=-\infty}^{+\infty} j^{-n} J_n(k\rho) e^{jn\varphi} \tag{14}$$

$$H_Z^s = H_0 \sum_{n=-\infty}^{+\infty} B_n j^{-n} H_n^2(k\rho) e^{jn\varphi} \tag{15}$$

where $B_n$ represents the unknown coefficient. It is shown that, in this case, only the components of $H_Z$, $E_\rho$ and $E\varphi$ have non-zero values and the other field components are null. Therefore, the magnetic field has no radial component and the waves can be considered $\mathrm{TM}\rho$.

$$E_\rho^i = \frac{1}{j\omega\varepsilon\rho}\frac{\partial H_z^i}{\partial\varphi} = \frac{H_0}{\omega\varepsilon\rho}\sum_{n=-\infty}^{+\infty} n j^{-n} J_n(k\rho) e^{jn\varphi} \tag{16}$$

$$E_\rho^s = \frac{1}{j\omega\varepsilon\rho}\frac{\partial H_z^s}{\partial\varphi} = \frac{H_0}{\omega\varepsilon\rho}\sum_{n=-\infty}^{+\infty} n j^{-n} B_n H_n^2(k\rho) e^{jn\varphi} \tag{17}$$

Now, the coefficients $B_n$ are obtained by applying the boundary condition (7).

$$B_n = -\frac{J_n(k\rho_0) + j(s-a)J_n'(k\rho_0)}{H_n^2(k\rho_0) + j(s-a)H_n'^2(k\rho_0)}, \quad n \neq 0 \tag{18}$$

Similar to Section 2.1, $B_0$ must be determined using additional information. By comparing the coefficients $A_n$ and $B_n$, it is observed that $B_n$ can be obtained from $A_n$ by replacing $a$ with $-a$. If $a = 0$ is selected, then $A_n$ and $B_n$ will be equal. For this polarization, $B_n$ coefficients for DB and D'B' are equal to PMC and PEC, respectively, which are also expressed in Table 1.

## 3. SCATTERING OF AN OBLIQUELY INCIDENT PLANE WAVE FROM MI CYLINDER

Similar to Section 2, oblique incidence to MI cylinder is investigated for two $\mathrm{TE}_Z$ and $\mathrm{TM}_Z$ polarizations.

### 3.1. Obliquely Incident Plane Wave: $\mathrm{TM}_Z$ Polarization

Assuming that a $\mathrm{TM}_Z$ plane wave traveling parallel to the $x$-$z$ plane is incident upon a cylinder of radius $\rho_0$, which is shown in Fig. 4. The incident electric field can be expressed as follows.

$$E^i = E_0 \left(\hat{a}_x \cos\theta_i + \hat{a}_z \sin\theta_i\right) e^{jk_0 z\cos\theta_i} e^{-jk_0 x\sin\theta_i} \tag{19}$$

Using (19) the $z$-axis component of the electric field can be obtained and expanded by an infinite sum of cylindrical wave functions in the following form

$$\begin{aligned} E_z^i &= E_0 \sin\theta_i e^{jk_0 z\cos\theta_i} e^{-jk_0 x\sin\theta_i} \\ &= E_0 \sin\theta_i e^{jk_0 z\cos\theta_i} \sum_{n=-\infty}^{n=+\infty} j^{-n} J_n(k_0\rho\sin\theta_i) e^{jn\varphi} \end{aligned} \tag{20}$$

By defining $E_0' = E_0 \sin\theta_i$, $G = e^{jk_0 z\cos\theta_i}$, $k_{0\rho} = k_0 \sin\theta_i$, $k_{0z} = k_0\cos\theta_i$ $E_z^i$ (20) is simplified to

$$E_z^i = E_0' G \sum_{n=-\infty}^{n=+\infty} j^{-n} J_n(k_{0\rho}\rho) e^{jn\varphi} \tag{21}$$

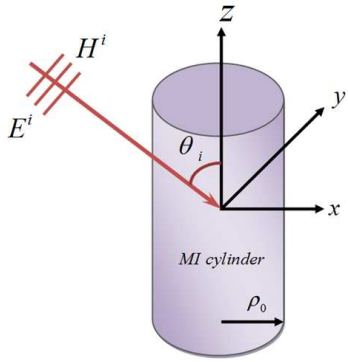


**Figure 4.** Uniform plane wave with oblique incidence to MI cylinder.

By using Maxwell equation, the radial components of electric and magnetic fields are equal

$$E_\rho^i = \frac{1}{k_\rho^2}\frac{\partial^2 E_z^i}{\partial\rho\partial z} = \frac{jk_{0z}E_0'G}{k_{0\rho}}\sum_{n=-\infty}^{n=+\infty} j^{-n}J_n'(k_{0\rho}\rho)e^{jn\varphi} \tag{22}$$

$$H_\rho^i = \frac{j\omega\varepsilon}{k_\rho^2}\frac{\partial E_z^i}{\rho\partial\varphi} = \frac{-k_0E_0'G}{\eta_0 k_{0\rho}^2}\sum_{n=-\infty}^{n=+\infty} nj^{-n}J_n(k_{0\rho}\rho)e^{jn\varphi} \tag{23}$$

In this case, because variations of electric field along $z$-axis are not zero ($\partial E = \partial z \neq 0$), both radial components of electric and magnetic fields exist. So there are two equations (6) and (7) for boundary conditions which must be satisfied. This means that there must be two unknown coefficients which are determined from boundary conditions. Therefore, cross-polarization fields are created in the scattered waves to satisfy the MI boundary upon the cylinder.

Considering the special case of MI boundary when $Z_{\mathrm{TE}} = Z_{\mathrm{TM}}$ (or isotropic impedance boundary) is another way that prove the existence of cross-polarization fields. As we know, in the oblique incidence to impedance cylinder cross-polarization fields are created to satisfy the impedance boundary condition. Therefore, the cross-polarization fields must be also created in the general form of impedance boundary (or MI boundary).

If the scattered fields in the $Z$ direction are expressed as

$$E_z^s = E_0'G\sum_{n=-\infty}^{n=+\infty} A_nH_n^2(k_{0\rho}\rho)e^{jn\varphi} \tag{24}$$

$$H_z^s = \frac{E_0'G}{\eta_0}\sum_{n=-\infty}^{n=+\infty} B_nH_n^2(k_{0\rho}\rho)e^{jn\varphi} \tag{25}$$

Then, the radial components of scattered electric and magnetic fields will be:

$$\begin{aligned} E_\rho^s &= \frac{-j\omega\mu}{k_\rho^2}\frac{\partial H_z^s}{\rho\partial\varphi} + \frac{1}{k_\rho^2}\frac{\partial^2 E_z^s}{\partial\rho\partial z} = \frac{k_0E_0'G}{k_\rho^2\rho}\sum_{n=-\infty}^{n=+\infty} nB_nH_n^2(k_{0\rho}\rho)e^{jn\varphi} \\ &\quad + \frac{jk_{0z}E_0'G}{k_{0\rho}}\sum_{n=-\infty}^{n=+\infty} A_nH_n'^2(k_{0\rho}\rho)e^{jn\varphi} \end{aligned} \tag{26}$$

$$H_\rho^s = \frac{j\omega\varepsilon}{k_\rho^2}\frac{\partial E_z^s}{\rho\partial\varphi} + \frac{1}{k_\rho^2}\frac{\partial^2 H_z^s}{\partial\rho\partial z} = \frac{-k_0E_0'G}{\eta_0 k_{0\rho}^2\rho}\sum_{n=-\infty}^{n=+\infty} nA_nH_n^2(k_{0\rho}\rho)e^{jn\varphi}$$

$$+\frac{jk_{0z}E_0'G}{k_{0\rho}\eta_0}\sum_{n=-\infty}^{n=+\infty}B_n{H'}_n^2(k_{0\rho}\rho)e^{jn\varphi} \tag{27}$$

For this case, the boundary conditions (6) and (7) can be written as

$$jk\left(H_\rho^i+H_\rho^s\right)-(s+a)\frac{1}{\rho}\frac{\partial\left(\rho\left(H_\rho^i+H_\rho^s\right)\right)}{\partial\rho}=0 \tag{28}$$

$$jk\left(E_\rho^i+E_\rho^s\right)-(s-a)\frac{1}{\rho}\frac{\partial\left(\rho\left(E_\rho^i+E_\rho^s\right)\right)}{\partial\rho}=0 \tag{29}$$

By substituting (22), (26), (26) and (27) in (28) and (29), the unknown coefficients $A_n$ and $B_n$ are obtained.

$$A_n=\frac{C_3C_5-C_2C_6}{C_1C_5-C_2C_4},\quad B_n=\eta_0\frac{C_1C_6-C_3C_4}{C_1C_5-C_2C_4} \tag{30}$$

where the coefficients $C_1$ to $C_6$ are defined as follows:

$$\begin{aligned}C_1 &= \frac{jk_{0z}k_{0\rho}}{k_0^2}\left(jk_0{H'}_n^2(k_{0\rho}\rho_0)-\frac{(s-a)}{\rho_0}\left({H'}_n^2(k_{0\rho}\rho_0)\right.\right.\\ &\quad\left.\left.+\rho_0k_{0\rho}{H''}_n^2(k_{0\rho}\rho_0)\right)\right) &(31)\\ C_2 &= \frac{n\eta_0}{k_{0\rho}\rho_0}\left(jk_0H_n^2(k_{0\rho}\rho_0)-(s-a)k_{0\rho}{H'}_n^2(k_{0\rho}\rho_0)\right) &(32)\\ C_3 &= \frac{-jk_{0z}k_{0\rho}}{k_0^2}j^{-n}\left(jk_0J_n'(k_{0\rho}\rho_0)-\frac{(s-a)}{\rho_0}\left(J_n'(k_{0\rho}\rho_0)\right.\right.\\ &\quad\left.\left.+\rho_0k_{0\rho}{J''}_n(k_{0\rho}\rho_0)\right)\right) &(33)\\ C_4 &= \frac{-n}{k_0\eta_0\rho_0}\left(jk_0H_n^2(k_{0\rho}\rho_0)-(s+a)k_{0\rho}{H'}_n^2(k_{0\rho}\rho_0)\right) &(34)\\ C_5 &= \frac{jk_{0z}k_{0\rho}}{k_0^2}\left(jk_0{H'}_n^2(k_{0\rho}\rho_0)-\frac{(s+a)}{\rho_0}\left({H'}_n^2(k_{0\rho}\rho_0)\right.\right.\\ &\quad\left.\left.+\rho_0k_{0\rho}{H''}_n^2(k_{0\rho}\rho_0)\right)\right) &(35)\\ C_6 &= \frac{n}{k_0\eta_0\rho_0}j^{-n}\left(jk_0J_n(k_{0\rho}\rho_0)-(s+a)k_{0\rho}J_n'(k_{0\rho}\rho_0)\right) &(36)\end{aligned}$$

By obtaining $A_n$ and $B_n$, the scattered far fields and then RCS can be calculated. By doing some simplification, the RCS in terms of the coefficients $A_n$ and $B_n$ are

$$\mathrm{RCS}=\lim_{\rho\to\infty}\left(2\pi\rho\left|\frac{E^s}{E^i}\right|^2\right)$$

$$= \frac{4}{k_{0\rho}}\left(\left|\sum_{n=-\infty}^{n=+\infty} A_n j^n e^{jn\varphi}\right|^2 + \left|\sum_{n=-\infty}^{n=+\infty} B_n j^n e^{jn\varphi}\right|^2\right) \tag{37}$$

Also, the ratio of cross-polarization to co-polarization fields at far field in terms of the coefficients $A_n$ and $B_n$ are

$$R_{cross_to_co} = \lim_{\rho\to\infty}\left|\frac{E^s_{cross}}{E^s_{co}}\right| = \frac{\left|\sum_{n=-\infty}^{n=+\infty} B_n j^n e^{jn\varphi}\right|}{\left|\sum_{n=-\infty}^{n=+\infty} A_n j^n e^{jn\varphi}\right|} \tag{38}$$

### 3.2. Obliquely Incident Plane Wave: $TE_Z$ Polarization

Similar to Section 3.1, the scattered fields can be also calculated for $TE_Z$ polarization. The incident and scattered fields are consider as

$$H^i_z = H'_0 G \sum_{n=-\infty}^{n=+\infty} j^{-n} J_n(k_{0\rho}\rho) e^{jn\varphi} \tag{39}$$

$$H^s_z = H'_0 G \sum_{n=-\infty}^{n=+\infty} A_n H^2_n(k_{0\rho}\rho) e^{jn\varphi} \tag{40}$$

$$E^s_z = -\eta_0 H'_0 G \sum_{n=-\infty}^{n=+\infty} B_n H^2_n(k_{0\rho}\rho) e^{jn\varphi} \tag{41}$$

By obtaining the radial components of electric and magnetic fields and applying boundary conditions the coefficients $A_n$ and $B_n$ are calculated.

$$A_n = \frac{D_3 D_5 - D_2 D_6}{D_1 D_5 - D_2 D_4}, \quad B_n = \frac{-1}{\eta_0}\frac{D_1 D_6 - D_3 D_4}{D_1 D_5 - D_2 D_4} \tag{42}$$

where the coefficients $D_1$ to $D_6$ are defined as follows:

$$D_1 = \frac{jk_{0z}k_{0\rho}}{k_0^2}\left(jk_0 H'^2_n(k_{0\rho}\rho_0) - \frac{(s+a)}{\rho_0}\left(H'^2_n(k_{0\rho}\rho_0) + \rho_0 k_{0\rho} H''^2_n(k_{0\rho}\rho_0)\right)\right) \tag{43}$$

$$D_2 = \frac{-n}{k_0\eta_0\rho_0}\left(jk_0 H^2_n(k_{0\rho}\rho_0) - (s+a)k_{0\rho} H'^2_n(k_{0\rho}\rho_0)\right) \tag{44}$$

$$D_3 = \frac{-jk_{0z}k_{0\rho}}{k_0^2} j^{-n}\left(jk_0 J'_n(k_{0\rho}\rho_0) - \frac{(s+a)}{\rho_0}\left(J'_n(k_{0\rho}\rho_0) + \rho_0 k_{0\rho} J''_n(k_{0\rho}\rho_0)\right)\right) \tag{45}$$

$$D_4 = \frac{n\eta_0}{k_0\rho_0}\left(jk_0H_n^2(k_{0\rho}\rho_0) - (s-a)k_{0\rho}H'^2_n(k_{0\rho}\rho_0)\right) \quad (46)$$

$$D_5 = \frac{jk_{0z}k_{0\rho}}{k_0^2}\left(jk_0H'^2_n(k_{0\rho}\rho_0) - \frac{(s-a)}{\rho_0}\left(H'^2_n(k_{0\rho}\rho_0) + \rho_0k_{0\rho}H''^2_n(k_{0\rho}\rho_0)\right)\right) \quad (47)$$

$$D_6 = \frac{-n\eta_0}{k_0\rho_0}j^{-n}\left(jk_0J_n(k_{0\rho}\rho_0) - (s-a)k_{0\rho}J'_n(k_{0\rho}\rho_0)\right) \quad (48)$$

Now, using (37) and (38), RCS and cross to co-polarization fields can be determined.

By considering the similarity between the coefficients $C_1$ to $C_6$ with $D_1$ to $D_6$, there seems to be a relationship between the unknown coefficients $A_n$ and $B_n$ in $\mathrm{TE}_Z$ and $\mathrm{TM}_Z$ polarizations. In $\mathrm{TM}_Z$ polarization, if $a$ is replaced with $-a$, it can be easily proved that the new coefficients of $A_n$ and $B_n$ are equal with coefficients of $A_n$ and $B_n$ for $\mathrm{TE}_Z$ polarization respectively. In other words, to obtain the unknown coefficients of $A_n$ and $B_n$ for $\mathrm{TE}_Z$ polarization, it is only coefficient to change $a$ to $-a$ for the coefficients of $A_n$ and $B_n$ in $\mathrm{TM}_Z$ polarization. In the special case of $a = 0$, the coefficients of $A_n$ and $B_n$ are equal for two polarizations. Normalized RCS and cross to co-polarization for boundary conditions of DB, D'B', PEC and PMC for both $\mathrm{TM}_Z$ and $\mathrm{TE}_Z$ polarization are plotted in Figs. 5 and 6, respectively.

As can be observed, RCS and cross to co-polarization for DB

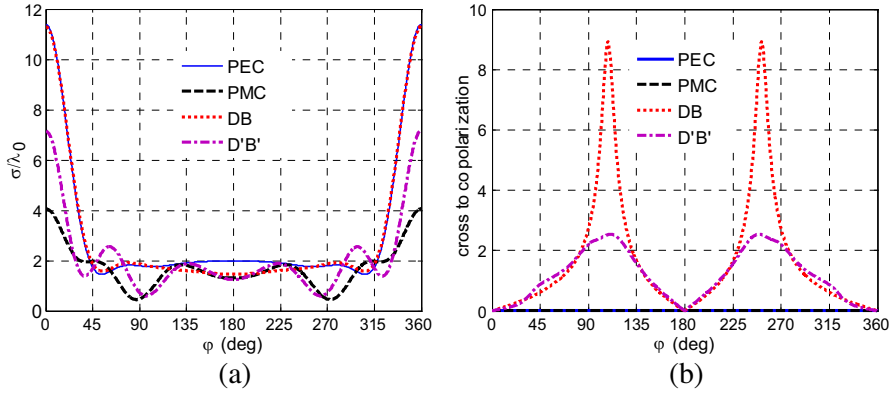


**Figure 5.** Normalized bistatic RCS and cross to co-polarization as a function of $\varphi$ for different boundary conditions for $\mathrm{TM}_Z$ polarization, $\theta_i = \pi/4$ and $\rho_0 = 0.6\lambda_0$.

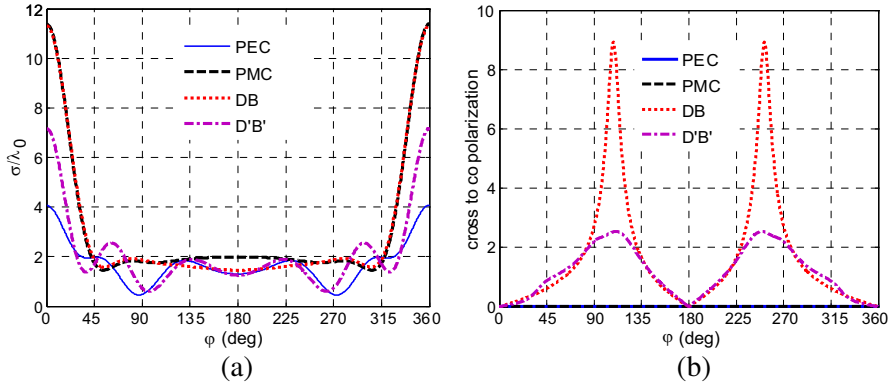


**Figure 6.** Normalized bistatic RCS and cross to co-polarization as a function of $\varphi$ for different boundary conditions for $TE_Z$ polarization, $\theta_i = \pi/4$ and $\rho_0 = 0.6\lambda_0$.

and D'B' boundaries are the same for both polarization. It happens since, for these boundaries, $a = 0$; therefore, RCS and cross to co-polarization are independent from type of polarizations. On the other hand, for PEC and PMC boundaries, $a$ has a non-zero value and therefore RCS has different behaviors for two polarizations. Another property observed in Figs. 5 and 6 is that cross polarization is created for oblique incidence to DB and D'B' cylinder. The cross polarization fields are functions of $\varphi$ and it can be proven in general case that, for all values of $s$ and $a$, cross-polarization is null in forward and backward directions.

### 3.3. The Optimum Choice of Boundary Conditions for Increasing or Decreasing the RCS

Considering that the aim is to minimize or maximize RCS in forward or backward directions and, if goal is desired for a specific polarization or both polarizations, the optimum boundary conditions can be chosen. If minimizing or maximizing the forward and backward RCS is desirable for both polarizations, a useful method is to select $a = 0$; therefore, RCS will be the same for both polarizations and the desired goal can be achieved by optimum choice of $s$. Normalized backward and forward RCS versus $s$ are plotted in Figs. 7(a) and (b) respectively. It can be observed that Normalized RCS changes in the range 2.5 to 32 for forward and 0.5 to 2.5 in the backward directions.

However, if the goal is to optimize the RCS for a particular

polarization, the two parameters of $s$ and $a$ can be chosen arbitrarily. For example, normalized forward and backward RCS for $TE_Z$ polarization are plotted in Fig. 8 for different values of $s$ and $a$. In this case, Normalized RCS changes in the ranges of 2.15 to 38.2 and 0.08 to 7.2 in forward and backward directions, respectively. Normalized RCS and cross to co-polarization versus $\varphi$ are plotted in Fig. 9 for different values of $s$ and $a$, which give the maximum and minimum values of the forward and backward RCS.

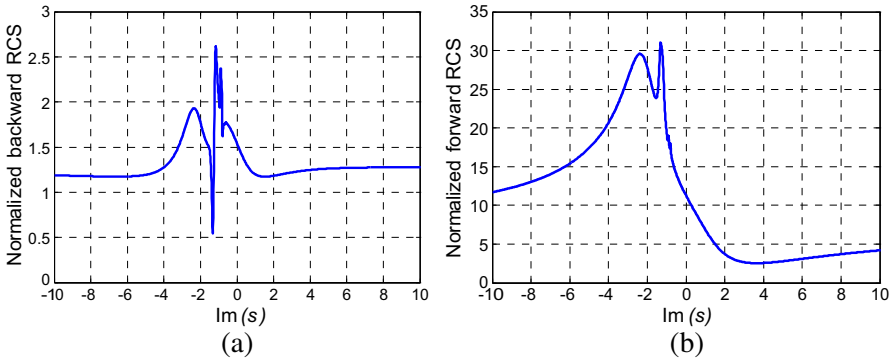


**Figure 7.** Normalized backward and forward RCS as a function of $-10 < \mathrm{Im}s < 10$. $\mathrm{Re}s = 0.02$, $a = 0$, $\theta_i = \pi/4$ and $\rho_0 = 0.6\lambda_0$. (a) Normalized backward RCS. (b) Normalized forwardRCS.

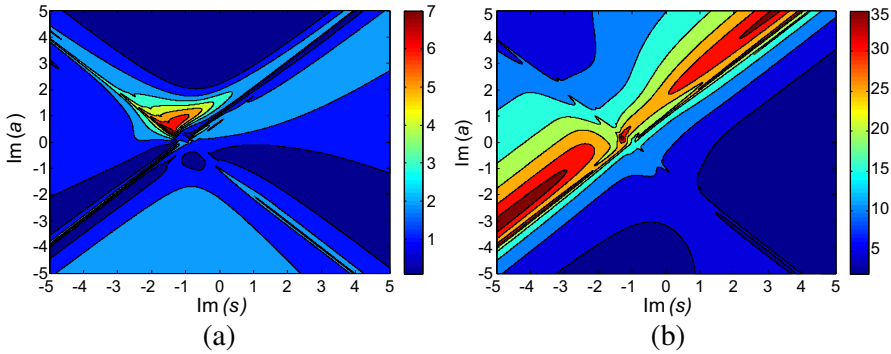


**Figure 8.** Normalized forward and backward RCS as a function of $-5 < \mathrm{Im}s, \mathrm{Im}a < 5$ for $TE_Z$ polarization. $\mathrm{Re}s = 0.02$, $\theta_i = \pi/4$ and $\rho_0 = 0.6\lambda_0$. (a) Normalized backward RCS. (b) Normalized forward RCS.

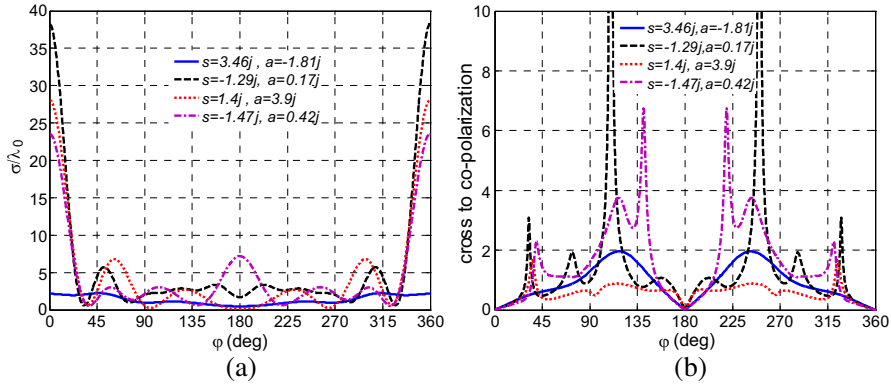


**Figure 9.** Normalized bistatic RCS and cross to co-polarization as a function of $\varphi$ for different values of $s$ and $a$ for $\mathrm{TE}_Z$ polarization, $\theta_i = \pi/4$ and $\rho_0 = 0.6\lambda_0$.

## 4. CONCLUSIONS

This paper investigated the problem of scattering from cylindrical structures with MI boundary conditions. Initially, the normally incident uniform plan wave to the MI cylinder was studied, and it was shown that this structure acted like an impedance cylinder with different surface impedances for two $\mathrm{TE}_Z$ and $\mathrm{TM}_Z$ polarizations. Then, oblique incidence to MI cylinder was investigated and it is observed that cross polarization was created in this case. It was demonstrated that DB and D'B' had cross polarization in oblique incidence and therefore could not act as PEC and PMC for $\mathrm{TE}_Z$ and $\mathrm{TM}_Z$ polarizations. This happened since, for both $\mathrm{TE}_Z$ and $\mathrm{TM}_Z$ polarizations, radial components of electric and magnetic fields existed. It was also shown that the forward or backward RCS can be significantly increased or decreased by selecting the optimum values of boundary conditions.

So far, various methods were presented for realizations of the DB and D'B' boundary in [6–10], However the realization of the MI boundary is still a challenge and is a topic for future study.

## REFERENCES

1. Hoppe, D. J. and Y. Rahmat-Samii, *Impedance Boundary Conditions in Electromagnetics*, Taylor & Francis, Washington, DC, 1995.

2. Lindell, I. V. and A. Sihvola, "Perfect electromagnetic conductor," *Journal of Electromagnetic Waves and Applications*, Vol. 19, No. 7, 861–869, 2005.
3. Kildal, P. S., "Artificially soft and hard surfaces in electromagnetic," *IEEE Trans. on Antennas and Propag.*, Vol. 38, No. 10, 1537–1544, 1990.
4. Lindell, I. V. and A. Sihvola, "Electromagnetic boundary conditions defined in terms of normal field components," *IEEE Trans. on Antennas and Propag.*, Vol. 58, No. 4, 1128–1135, Apr. 2010.
5. Lindell, I. V. and A. Sihvola, "Uniaxial IB-medium interface and novel boundary conditions," *IEEE Trans. on Antennas and Propag.*, Vol. 57, No. 3, 694–700, Mar. 2009.
6. Lindell, I. V. and A. Sihvola, "Electromagnetic boundary condition and its realization with anisotropic metamaterial," *Phys. Rev. E*, Vol. 79, No. 2, 026604-7, 2009.
7. Lindell, I. V. and A. Sihvola, "Simple skewon medium realization of DB boundary conditions," *Progress In Electromagnetics Research*, Vol. 30, 29–39, 2012.
8. Zaluški, D., D. Muha, and S. Hrabar, "Numerical investigation and possible realization of metamaterial-based DB boundary surface," *Proc. on ICECOM*, Dubrovnik, Croatia, 251–253, 2010.
9. Lindell, I. V. and A. Sihvola, "Zero axial parameter (ZAP) sheet," *Progress In Electromagnetics Research*, Vol. 89, 213–224, 2009.
10. Lindell, I. V., A. Sihvola, L. Bergamin, and A. Favaro, "Realization of the D'B' boundary condition," *IEEE Antennas Wireless Propag. Lett.*, Vol. 10, 643–646, 2011.
11. Wallén, H., I. V. Lindell, and A. Sihvola, "Mixed-impedance boundary conditions," *IEEE Trans. on Antennas and Propag.*, Vol. 59, No. 5, 1580–1586, May 2011.
12. Lindell, I. V., A. Sihvola, P. Ylä-Oijala, and H. Wallén, "Zero backscattering from self-dual objects of finite size," *IEEE Trans. on Antennas and Propag.*, Vol. 57, No. 9, 2725–2731, Sep. 2009.
13. Balanis, A., *Advanced Engineering Electromagnetic*, John Wiley & Sons, 1989.